www.czasopisma.pan.pl PAN POLSKA AKADEMIA NAUK www.journals.pan.pl

Arch. Metall. Mater. **68** (2023), 2, 697-701

DOI: https://doi.org/10.24425/amm.2023.142451

T. BULZAK[1*]

MULTI WEDGE CROSS ROLLING OF AXLE FORGINGS

This paper presents the results of research into the cross wedge rolling (CWR) process of axle forgings. The presented results concern the parallel rolling process with two wedges. The use of two parallel wedges is aimed at shortening the tool length (increasing productivity) and reducing the values of wedge opening angles and increasing the forming angles, so that the condition $0.04 \leq \mathrm{tg}\alpha\,\mathrm{tg}\beta \leq 0.08$ is maintained to guarantee the highest quality forgings. The article analyses the influence of the design of the double wedge tool on the geometric correctness of the forgings obtained, the value of the failure criterion and the force parameters of the process. The results obtained show that the use of multi wedge tools improves rolling conditions by increasing productivity and reducing the tendency of the material to crack with appropriately selected tool parameters.

Keywords: cross wedge rolling; fracture; multi wedge tools; FEM; axles

1. Introduction

Cross wedge rolling (CWR) is a technology that enables the production of axisymmetric elongated products. This technology is used in the production of forgings used in drop forging technology [1,2]. In many cases, finished shaft and axle forgings are produced using this technology [3,4]. In spite of many completed studies, CWR technology still suffers from the main problem, which is cracking of the rolled material [5,6]. In the case of long products such as railway axles, whose length is more than 10 times the maximum diameter, the length of the wedge tool is a significant limitation. Long forgings require the use of tools of considerable size, which in many cases cannot be used due to the limited size of rolling mills. Therefore, in order to shorten the tool length, large spreading angle β values are used. On the one hand, increasing the spreading angle β shortens the tool length, but on the other hand, it significantly increases the risk of material cracking during rolling [7,8]. With large spreading angle β values, it is recommended to use the smallest possible forming angles α so that the condition of $0.04 \leq \mathrm{tg}\alpha\,\mathrm{tg}\beta \leq 0.08$ is fulfilled [9,10]. Meeting the aforementioned condition ensures stable realization of the rolling process without slips and eliminates the phenomenon of material lapping during the rolling process. On the other hand, at minimum values of the forming angle α, the risk of material cracking increases significantly [11].

This paper presents the results of a cross wedge rolling test using a tool with two parallel wedges. The use of two wedges makes it possible to use smaller angle β values on each wedge. In addition, the smaller angle β values make it possible to use larger angle β values at which the condition $0.04 \leq \mathrm{tg}\alpha\,\mathrm{tg}\beta \leq 0.08$ is fulfilled.

2. Materials and methods

In the study, the axle was rolled using a dual wedge tool shown in Fig. 1. The study was carried out with varying geometric parameters of the dual wedge tool. The tool design variants analysed are summarised in TABLE 1. During the CWR process, a ϕ33 mm diameter and 203.9 mm long section was rolled in the central zone of the axis. The initial diameter of the billet bar was ϕ38 mm.

Numerical simulations of the problem analysed were carried out using the finite element method. Simufact Forming software was used for numerical modelling. The geometrical model of the analysed problem is presented in Fig. 2. The numerical model consists of two flat tools and a billet. The bottom tool remains stationary, while the top tool moves at a constant velocity of 300 mm/s. The rolled material was modelled as a rigid-plastic object using 3D 8-node hexagonal elements (Hex 8) with an average size of 1.25 mm. Remeshing of the finite element mesh

[1] LUBLIN UNIVERSITY OF TECHNOLOGY, FACULTY OF MECHANICAL ENGINEERING, DEPARTMENT OF METAL FORMING, 36 NADBYSTRZYCKA STR., 20-618, LUBLIN, POLAND

* Corresponding author: t.bulzak@pollub.pl

TABLE 1

Set of geometric parameters of the analysed tools

No.	α_1 [°]	α_2 [°]	$2\beta_1$ [°]	$2\beta_2$ [°]	β [mm]
1	22.5	22.5	13.69	22.84	60
2	22.5	22.5	12.78	23.78	56
3	22.5	22.5	11.42	19.06	60
4	22.5	22.5	10.66	19.82	56
5	20	20	17.06	28.5	75
6	20	20	14	28.5	75
7	20	20	15.94	29.67	70
8	20	20	12	29.67	70
9	20	20	14.25	23.79	75
10	20	20	12	23.79	75
11	20	20	13.31	24.76	70
12	20	20	11	24.76	70
13	22.5	22.5	11.87	24.69	52
14	22.5	22.5	9.91	20.58	52
15	20	20	15.04	30.58	66
16	20	20	12.55	25.53	66
17	20	20	10	25.53	66
18	22.5	22.5	8.17	24.51	50
19	30	25	8.17	22.17	50
20	30	25	7.36	22.99	44.5
21	25	25	7.31	21.69	53

was initiated when the effective strain value increased by 0.4. The rheology of the rolled C35 steel material was described by the equation:

$$\sigma_f = 4585.91 \cdot e^{-0.00363T} \cdot \varepsilon^{-0.000194T+0.04895} \cdot \cdot e^{\frac{-1.1162e-5-0.03678}{\varepsilon}} \cdot \dot{\varepsilon}^{0.0001905T-0.0458} \quad (1)$$

where: σ_f – flow stress, ε – effective strain, $\dot{\varepsilon}$ – effective strain rate, T – temperature. A rheological model of C35 steel was developed based on the results of experimental tests carried out in the compression test on a Gleeble thermomechanical simulator. The tests were carried out at 1000°C, 1100°C and 1200°C. The specimens were compressed at three strain rates of: 0.1 s^{-1}, 1 s^{-1}, and 10 s^{-1}.

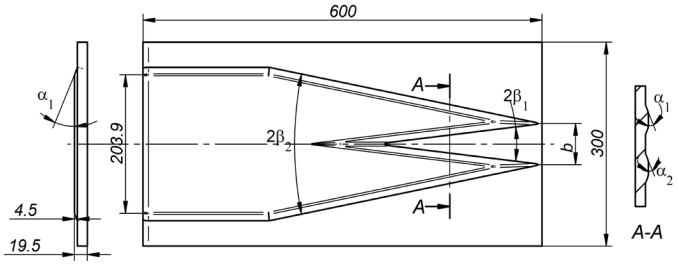

Fig. 1. Two wedge tool concept

The rolling process was carried out under hot forming conditions. The initial billet temperature was 1150°C, while the tool temperature was constant at 50°C. The heat transfer coefficient between the billet and the tools was 20 kW/m^{2}K, while the heat transfer coefficient between the billet and the environment was 0.2 kW/m^{2}K. The friction conditions between the billet and tools were described by the Tresca friction model, for which the friction factor was m = 0.8.

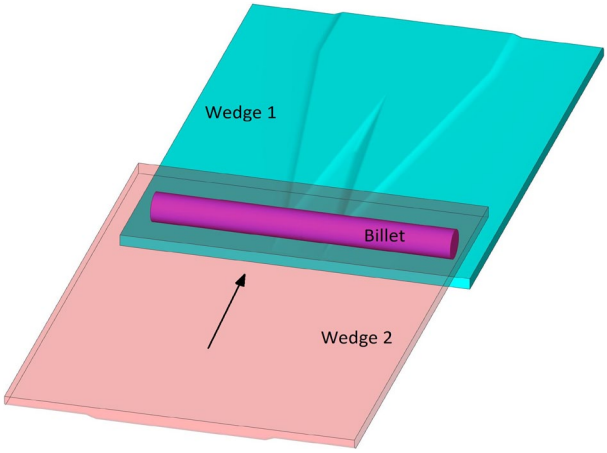

Fig. 2. Geometrical model of a multi wedge cross rolling

3. Result and discussion

Fig. 3 presents a histogram showing the value of the damage function calculated according to the normalised Cockcroft-Latham (CL) criterion. The smallest value of the damage function occurred for case no. 3, while the highest value occurred for case no. 15. Using regression analysis, a mathematical model was developed to describe the relationship CL = $f(\alpha_1, \alpha_2, \beta_1, \beta_2, b)$. It is a statistically significant model (Fisher F statistic = 38.511; p = 2,3966e-07). The quality of fit of the developed mathematical model expressed by the coefficient of determination R^2 is 0.93 and adjusted coefficient of determination $\bar{R}^2$ is 0.91. The developed model is expressed by the following equation:

$$CL = -2.12 + 0.124\alpha_1 - 0.168\alpha_2 + 0.111\beta_1 + + 0.294\beta_2 + 0.035b \quad (2)$$

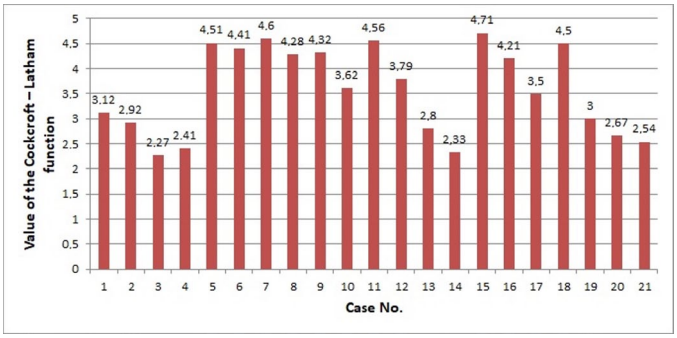

Fig. 3. Maximum values of the damage function calculated according to the normalised Cockcroft-Latham criterion for the analysed cases

Fig. 4 graphically shows the error values between the damage function values calculated using the normalised Cockcroft-Latham criterion in FEM and the mathematical model described

by equation (2). For most of the cases analysed, the relative error value is below 10%. The largest error value was recorded for case 18, where the relative error was around 40%. The reason for such a high error value in this one case is difficult to find, as the die parameters for this case do not differ significantly from those of other dies. The most likely cause in this case is a numerical error that overestimated the value of the damage function in the FE simulation. The average value of the absolute error for the built model from all cases analysed is 0.27, while the average value of the relative error was 7.01%. It can be concluded that the obtained mathematical model predicts well the values of the damage function during multi-wedge cross wedge rolling with two wedge tools.

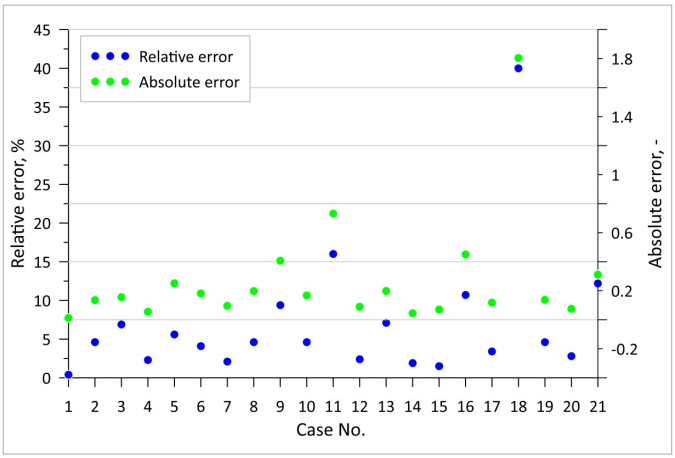

Fig. 4. Comparison of errors between damage function values calculated with the normalised Cockcroft-Latham criterion in FEM and the mathematical model equation (2)

Fig. 5 shows colour maps showing the distribution of the damage function for the most favourable case No. 3 and the least favourable case No. 15. In both cases shown in Fig. 5 the maximum values of the damage function are located in the central zone of the forging. For case No. 3 the area of the occurrence of the maximum values of the damage function is much larger compared to the area of the maximum values of the damage function in case No. 15. In the forging rolled with tool set No. 15, a pronounced roughening can be observed in the central part, where the maximum values of the damage function are located. This roughening is the result of too much material being enclosed between the wedges, which caused overfilling of the cavity created by the two tool segments. As a result of the overfilling of the cavity, intensive ovalization of the cross-section took place, which promoted an increase in the stress state and strain in the central part. The effect of this overfilling is an increase in the value of the damage function.

Fig. 6 shows an isometric view of the rolled forgings for case No. 3 and 15. For both forgings shown in Fig. 6, a pronounced roughening can be observed in the central zone of the rolled step of the forgings. In the case of the forging rolled with tool set No. 3, the roughening of the material in the central zone is much less than for the forging rolled with tool set No. 15. Ovalization of the section in the central zone of the forging will undoubtedly affect the value of plastic strain, stress state and force parameters of the rolling process.

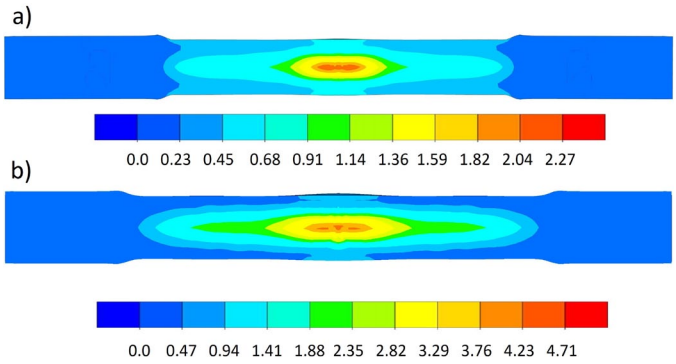

Fig. 5. Distribution of damage functions according to Cockcroft-Latham criterion: a) case No. 3, b) case No. 15

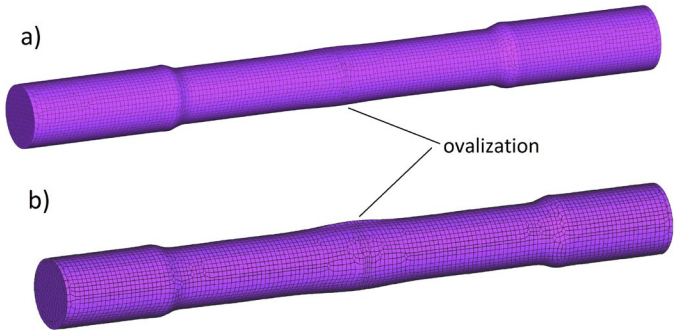

Fig. 6. Isometric view of forgings: a) case no. 3, b) case no. 15

Fig. 7 shows the distribution of plastic strain in forgings rolled with tool set No. 3 and 15. In both forgings, the maximum values of strain are located in the central zone in the area where material roughening was observed. The increase in strain in this area is a result of excessive compression of the material during removal of section ovalization in the tool calibration zone. Significantly higher values of strain were observed in the forging rolled with tool set No. 15. This is due to the fact that for this forging, significantly greater material roughening was observed in the central part of the forging. The increase in plastic strain in this area of the forging is also responsible for the increase in the value of the damage function.

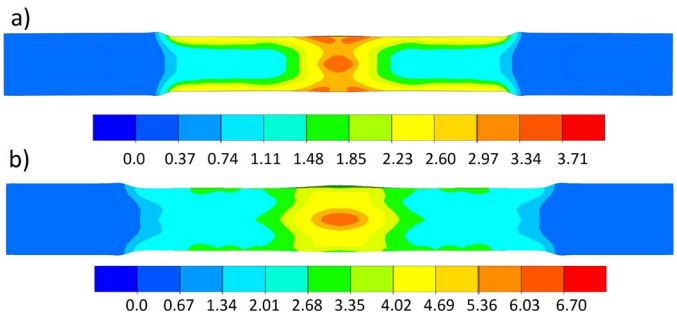

Fig. 7. Distribution of effective plastic strain: a) case No. 3, b) case No. 15

Fig. 8 shows the changes in the maximum principal stress in the central part of the rolled forgings. It can be seen from the presented graph that in the initial stage of rolling the changes in the stress values for both cases are identical. For both rolling cases, the maximum stress value occurs around 1.5 s of the process duration. For tool set No. 15, the maximum stress value is slightly higher. After reaching the maximum value, the stress begins to decrease. When rolling with tool set No. 3 in the calibration zone of the forging, the stress value is set at a constant level of about 40 MPa. In the case of tool set No. 15, a rapid increase in stress to a value of about 60 MPa can be observed at 2 s of the process duration, which is associated with intensive compression of the roughening material formed in the central part of the forging. In the calibration zone of tool set No. 15, the maximum principal stress assumes a variable character, which is due to the removal of excessive ovalisation caused by the roughening of the material in the central part of the forging. In summary, the overfilling of the cavity between the wedges promotes an increase in stress and strain, resulting in an excessive increase in the value of the damage function.

Fig. 9 presents a histogram showing the maximum values of the rolling force for the analysed rolling cases. It can be seen from the presented data that the lowest rolling force occurred for tool set No. 3, while the highest rolling force was recorded for case No. 15. The values of maximum and minimum rolling forces were recorded for the same cases, in which the minimum and maximum values of the damage function were recorded. It can therefore be concluded that the amount of material roughening in the central zone of the forging is reflected identically in the damage function values as well as in the rolling force values. The greater the roughening of the material in the central area of the forging, the greater the rolling resistance of the material.

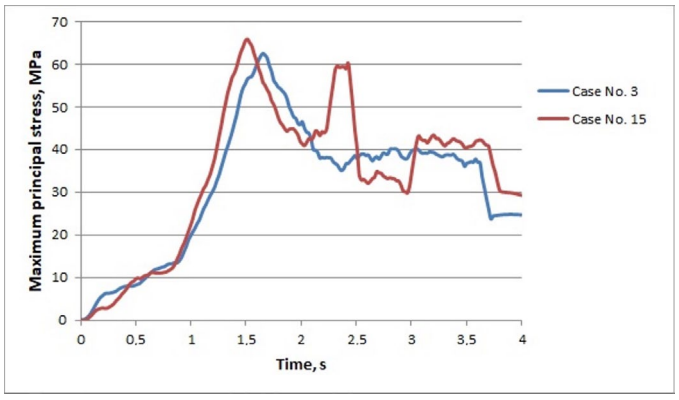

Fig. 8. Variations in maximum principal stress during rolling

TABLE 2 summarises the correlation coefficients between the geometrical parameters of the tool and the value of the damage function and the value of the rolling force. From the data presented, it can be seen that all variables describing the tool geometries have a significant effect on both the value of the damage function and the value of the maximum rolling force.

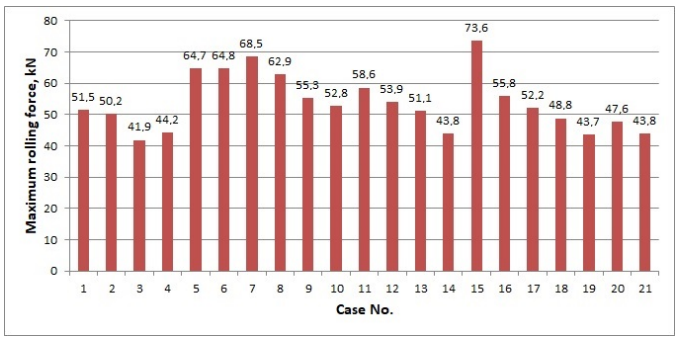

Fig. 9. Maximum values of the rolling force for the analysed cases

There is a negative correlation between the formation angles α_1, α_2 and both the damage function and the maximum rolling force values. This means that an increase in the values of these angles will result in a decrease in the value of the damage function and the maximum rolling force. The remaining explanatory variables have positive correlations. Angle β_2 has the greatest influence on the value of the damage function CL, while angles α_1 and β_1 have the least influence. In the case of the maximum rolling force, angle β_2 also has the greatest influence on this parameter. The maximum rolling force is least influenced by the value of angle α_1.

TABLE 2

Correlation table between wedge tool parameters and values of damage function and force

	α_1	α_2	β_1	β_2	b
CL	–0.59836	–0.74915	0.599201	0.833454	0.692588
Force	–0.60426	–0.74027	0.77557	0.946468	0.694308

4. Conclusion

This paper examines the process of long-axis cross-wedge rolling using a tool equipped with two parallel wedges. The following conclusions were drawn on the basis of the study:

- using two wedges in parallel, there is a high risk of incomplete rolling of the forging, which manifests itself by thickening of the material in the central part,
- the greater the roughening of the forging that occurs during rolling, the greater the risk of internal cracks forming,
- in order to reduce the value of the damage function, it is recommended to use the lowest possible values for the following parameters, β_1, β_2 and b that characterise the geometry of the multi wedge tool,
- for angle α_1 α_2, it is recommended to use the largest possible values for this parameter in order to reduce the value of the damage function,
- the influence of the parameters characterising the geometry of the multi wedge tool on the maximum value of the rolling force is identical to that of the damage function.

Acknowledgement

The research was financed in the framework of the project: Development of new rolling technologies for rail axle forgings, No. LIDER/9/0060/L-12/20/NCBR/2021. Total cost of the Project: 1 466 831.25 PLN. The project is financed by the National Centre for Research and Development under the 12th edition of the LIDER Programme.

REFERENCES

[1] B. A. Behrens, M. Stonis, T. Blohm, J. Richter, Int. J. Mater. Form. **11**, 67-76 (2018).

[2] J. Li, B. Wang, S. Fang, P. Chen, Int. J. Adv. Manuf. Technol. **108**, 1827-1838 (2020).

[3] T. Bulzak, Z. Pater, J. Tomczak, Arch. Civ. Mech. Eng. **17** (4), 729-737 (2017).

[4] Z. Pater, J. Tomczak, T. Bulzak, Strength Mater. **49**, 521-530 (2017).

[5] X. Zhou, Z. Shao, C. Zhang, F. Sun, W. Zhou, L. Hua, J. Jiang, L. Wang, Int. J. Mach. Tools Manuf. **159**, 103647 (2020).

[6] T. Bulzak, Materials. **14** (21), 6638 (2021).

[7] Z. Pater, J. Tomczak, T. Bulzak, J. Mater. Res. Technol. **9** (6), 14360-14371 (2020).

[8] C. Yang, H. Dong, Z. Hu, J. Mater. Process. Technol. **252**, 322-332 (2018).

[9] Z. Pater, J. Tomczak, T. Bulzak, Arch. Civ. Mech. Eng. **18** (1), 149-161 (2018).

[10] Z. Pater, J. Mater. Process. Technol. **164-165**, 1235-1240 (2005).

[11] H. Ji, J. Liu, B. Wang, Z. Zhang, T. Zhang, Z. Hu, J. Mater. Process. Technol. **221**, 233-242 (2015).